

AD-A102 236

NAVAL RESEARCH LAB WASHINGTON DC
SATELLITE SHIELDING USING SECTOR ANALYSIS. (U)
AUG 81 J B LANGWORTHY

F/6 22/2

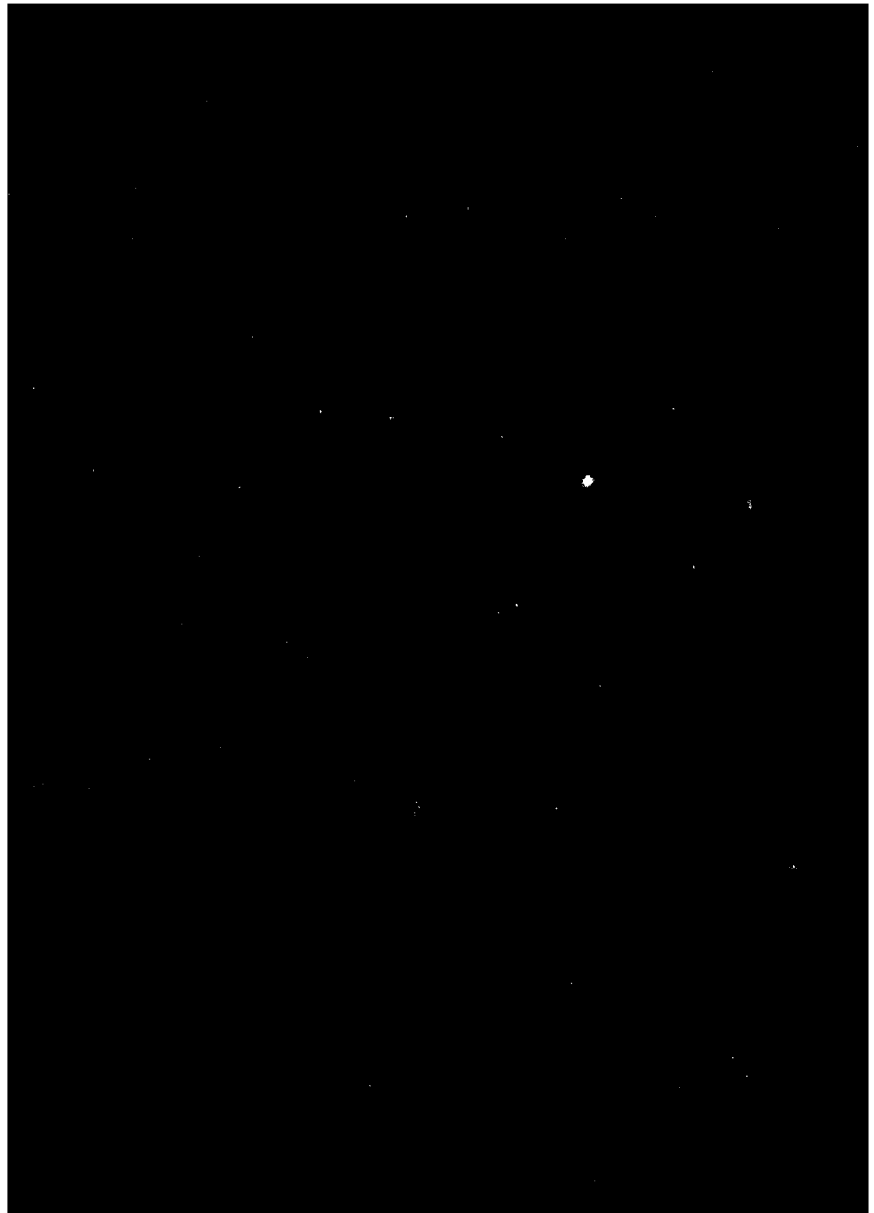
UNCLASSIFIED

NRL-WR-4577

NL

1 of 1
AD-A102 236

END
DATE
FILED
8-81
DTIC



SECURITY CLASSIFICATION OF THIS PAGE (When Data Entered)

REPORT DOCUMENTATION PAGE			READ INSTRUCTIONS BEFORE COMPLETING FORM
1. REPORT NUMBER <i>(1) N71-MR-</i> NRL Memorandum Report 4577	2. GOVT ACCESSION NO. <i>AD-A142 236</i>	3. RECIPIENT'S CATALOG NUMBER	
4. TITLE (and Subtitle) SATELLITE SHIELDING USING SECTOR ANALYSIS	5. TYPE OF REPORT & PERIOD COVERED Interim report on a continuing NRL problem.		
6. AUTHOR(s) <i>J. B. Langworthy</i>	7. PERFORMING ORGANIZATION NAME AND ADDRESS Naval Research Laboratory Washington, DC 20375		
8. PERFORMING ORGANIZATION NAME AND ADDRESS <i>11 August 1981</i>	9. PROGRAM ELEMENT, PROJECT, TASK AREA & WORK UNIT NUMBERS 61153N; RR012-01-41; 66-0439-0-1		
10. CONTROLLING OFFICE NAME AND ADDRESS <i>11 August 1981</i>	11. REPORT DATE August 11, 1981		
12. NUMBER OF PAGES 27	13. SECURITY CLASS. (of this report) UNCLASSIFIED		
14. MONITORING AGENCY NAME & ADDRESS (if different from Controlling Office) <i>11 August 1981</i>	15. DECLASSIFICATION/DOWNGRADING SCHEDULE		
16. DISTRIBUTION STATEMENT (of this Report) <i>11 August 1981</i>	17. DISTRIBUTION STATEMENT (of the abstract entered in Block 20, if different from Report)		
18. SUPPLEMENTARY NOTES			
19. KEY WORDS (Continue on reverse side if necessary and identify by block number) Satellite shielding Electron shielding Proton shielding Sector analysis dose			
20. ABSTRACT (Continue on reverse side if necessary and identify by block number) Satellite shielding methods previously developed and previously applied for fission beta electron spectra are here extended by application to natural earth belt spectra including protons. They are also extended by application to individual electronic device shielding. The previous numerical results are changed by recalibration of the electron dose code BRAND. This and other code improvements are reported. In the device shielding, comparison is made with other published work.			

DD FORM 1 JAN 73 1473

EDITION OF 1 NOV 68 IS OBSOLETE
S/N 0102-014-6601

SECURITY CLASSIFICATION OF THIS PAGE (When Data Entered)

25-12-8

OK

Accession For	
NTIS GRA&I	
DTIC TAB	
Unpublished <input type="checkbox"/>	
Justification _____	
By _____	
Distribution/ _____	
Availability Codes	
Dist	Avail and/or Special
A	

TABLE OF CONTENTS

I. Introduction	1
II. Code Developments	2
A. The Shield Mass Distribution	2
B. The Spectrum and Dose Integrals	3
C. Possible Improvements	7
D. Recalibration	7
E. Proton Dose	9
III. The Effects of Calibrating BRANDE to Agree With SHIELDOSE	10
IV. Fission Beta Shield Effectiveness Against Natural Fluences	15
V. Device Shielding for Various Spectra	19
Acknowledgments	24
References	25

FIGURES

1. Ideal Dose Point Near a Face	3
2. Mass Distribution Test	4
3. Model Geometry Dose-Depth Relations	11
4. Doses Before Shielding	12
5. Doses With Shielding	13
6. Comparison of Electron Spectra	20
7. CMOS Position in Inertial Measurement Unit	22
8. Comparison of Mass Distributions	23

TABLES

I. Ratio of Corner Dose to Face Dose	10
II. Recalibrated Doses at 28 Test Points	14
III. Satellite Structure Doses for Natural Spectra	16
IV. Dose Reductions Due to Fission Beta Shield	17
V. Device Dose Reduction Factors	24

SATELLITE SHIELDING USING SECTOR ANALYSIS

I. Introduction

A demonstration of techniques necessary in shielding a satellite against weapon-injected electrons was completed in December 1978. A report¹ (hereafter SS) has since been published. The central tools of this work are the codes SECTOR, BRANDE and PROTON produced by J. Janni and G. Radke of the Air Force Weapons Laboratory (AFWL), Albuquerque, NM. These codes calculate dose at a point in a complex geometry using sector analysis. For a more detailed description of the first two codes, refer to SS.

The report SS expressed a concern about the effects of the approximations made in the use of sector analysis. Since then, two year's work on (discussed in Section II) and with these codes has considerably increased their usefulness and the author's familiarity with them. As it happens no instance of an inadequacy attributable to sector analysis has been found up to this time. This report will offer a few more descriptive details and allay some potentially misleading implications of SS. The report SS also expressed concern about the adequacy of calibration. In fact, recalibration has made significant changes to the numerical results of SS which will be given in Section III. Applications which extend the results of SS to other threats and spectra are reported in Sections IV and V. Also Section V makes a comparison with AFWL work.

Because concern has been expressed about sector analysis, it may be worthwhile to make two comments on what may be expected in theory and in practice. First, sector analysis is a kind of straight-ahead approximation which is better at higher energies and for heavier particles. While one may expect it to be poor for electrons much below one MeV, sizeable effects are apparently not observed and may be obviated by solid angle averaging, at least to the accuracy of 15% used so far. Secondly, the electron dose calculation utilizes only single material range and transmission information. Thus build-up and dose-enhancement effects are omitted and one must expect dose within a few mils of any interface to be subject to large errors. In shielding calculations such errors and those due to omitting bremsstrahlung may be largely avoided by confining one's interest to acceptable depths of shield. The calibration to be described is for aluminum shield and aluminum detector, and there has been no estimate of error for the use of other materials.

II. Code Developments

Each actual code change to be mentioned in this section has been motivated by needs of the work to be reported in the last three sections of this report. Subsection C reports potential changes only. The last subsection is the only one not dealing with BRANDE. Use of the shielding mass distribution is made in Section V. Use of the integration improvements and recalibration is made in all three sections, but historically the necessity of better integration was not forced until comparisons of dose from different spectra were required and recalibration became convenient only with the availability of a new standard.

A. The Shield Mass Distribution

Augmenting BRANDE by adding graphical output of the shielding mass distribution about some dose point was straightforward. The ordinate of this type of graph (see Fig. 2) is fraction of the total solid angle (4π sr) and the abscissa is shield thickness. The geometry represented may be visualized by assigning the area above the curve to shield and the area below to void. The plot is an accumulated distribution, so a point on this plot means: this (ordinate) solid angle contains all shield with less than this (abscissa) thickness. It is expressible as an integral

$$w(T) = \int_0^T \frac{dw}{dt} dt$$

where T is the thickness plotted, t is the thickness variable, and dw/dt is the solid angle in the thickness interval $(t, t+dt)$. In sector analysis a convenient discrete rendition would be

$$f_n = \frac{\Delta t}{N} \sum_{k=1}^n s_k$$

where s_k is the number of sectors in the thickness bin at $t_k = k\Delta t$ assuming bins of constant thickness Δt , N is the total number of sectors, and f_n is the fraction of total solid angle included in n bins. In implementing this, it was first necessary to sort sectors by thickness. A smoothing procedure was added by lumping thicknesses which are equal within plotting tolerance into a single solid angle bin and plotting this at bin center. To avoid artificial irregularities it was also found useful to offset the fixed sectoring grid from the symmetry axes of regular figures.

In order to test this output the results for a dose point at a given depth in the center of one face of a rectangular parallelepiped (RPP) were compared with that calculated for such a point, slightly idealized. Consider a point at depth t_0 in a semi-infinite medium. Taking the Z axis perpendicular to the face, the solid angle between two cones separated

by da at polar angle a is

$$dw = 2\pi \sin a da.$$

The shield thickness there is

$$t = t_0 \sec a$$

$$\text{so } dt = t_0 \sec a \tan a da,$$

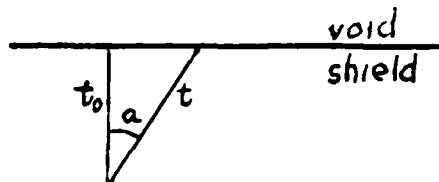


Fig. 1. Ideal dose point near a face.

hence

$$\frac{dw}{dt} = \frac{2\pi}{t_0} \cos^2 a = \frac{2\pi t_0}{t^2}$$

and

$$w(t) = 2\pi t_0 \int_{t_0}^t t^{-2} dt = 2\pi \left(1 - \frac{t_0}{t}\right).$$

The fraction of solid angle is

$$f(t) = \frac{1}{2} \left(1 - \frac{t_0}{t}\right).$$

This distribution for an ideal face point is plotted in Fig. 2. The result from the augmented version of BRANDE is also plotted and agrees fairly well, oscillating on both sides of the ideal distribution. This error would be larger had the sectoring grid not been offset and is a sampling error produced by grid symmetries. This error could be reduced by using more sectors than the 120 used in this test.

The SS work showed the utility of analyzing shielding problems in terms of the three ideal geometries for dose points: face, dihedral, and trihedral points. Distributions for the latter two points on the same RPP are also plotted in Fig. 2. It is probably obvious that each distribution asymptotically approaches the solid angle exposure of each geometry: 0.5, 0.75, and 0.875 respectively. This demonstrates the utility of the mass distribution diagram as a tool which discriminates gross aspects of geometry while averaging over details. It should be noted that BRANDE ignores thicknesses of greater than 5.0 g/cm² in calculating dose. In fact for the geometry described in Section V using the Carter spectrum, 96.6% of the dose is contributed by thicknesses below 1.5 g/cm². The related mass distribution is the solid line in Figure 8.

B. The Spectrum and Dose Integrals

Often spectra are available in either of two forms, integral or differential, but not both. Ordinarily it would be supposed that this poses no problem. However the spectra typically show negative exponential

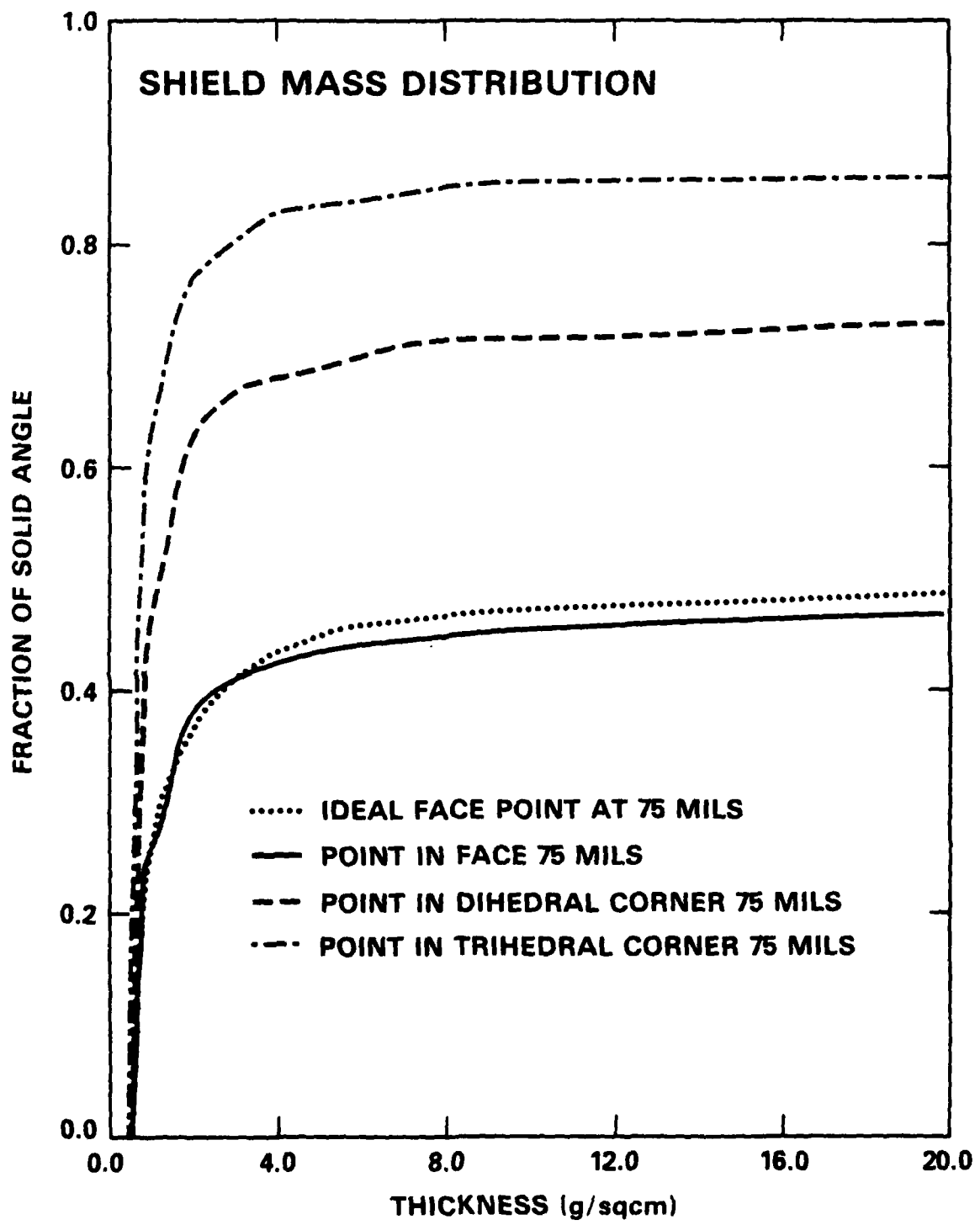


Fig. 2 — Mass distribution test

or power law character and vary over several orders of magnitude of electron fluence in the energy range of interest, say 0.1 to 8.0 MeV. Because of this strong variation, end point errors at low energy may be too large to handle by ordinary means. Application of naive integration methods to these problems has been observed to give errors of a factor of 3 or more. Therefore in order to justify comparison of doses from spectra given in different forms it is necessary to reconcile the integration methods. Actually this difficulty occurred in the worst case, that of the spectrum normalization integral, which is required only when the differential spectrum is given. Other integral requirements, those of the average energy or of dose, are not as stringent since the integrand is zero or nearly so at low energy. These last two integrals may have problems at high energy. If so the best remedy is to move the high energy end point up far enough to avoid the difficulty.

General consideration of the dependence of an integral on its end points reveals a flaw in a typical statement of a man-made fluence scenario. Thus it might be stated that a certain event produces a total electron fluence of 10^{16} cm^{-2} . This statement is susceptible of an interpretation error unless there is an understanding of the low energy end point. Zero energy may be understood but is seldom actually used since such a spectrum would have much fluence which contributed nothing in most cases of interest. Very approximately, the comparative error made using the Carter fission beta spectrum by having differing low energy end points is 7% for each 0.1 MeV difference if one of the end points is near 0.1 MeV.

In order to calculate dose from the dose conversion factors, $\delta(E)$, which are output from BRANDE as a table over a range of specified energies, E , one needs to perform the integral

$$D = \int_{E_2}^{E_1} \delta(E) \phi(E) dE$$

where $\phi(E)$ is the differential electron spectrum. A spectrum may be described by stating a table of $\phi(E)$ (denoted by DS), or, more conveniently for many purposes, by tabulating the accumulated spectrum (AS),

$$N(E) = - \int_{E_2}^E \phi(E) dE.$$

Since ϕ is of negative exponential character, one takes $E < E_2$ so that $N(E)$ is the number of electrons with energy greater than E . The opposite procedure would cause small numbers to be added to large, resulting in loss of significance. Often only relative dose is of interest, in which case the spectrum normalization or total fluence needs to be removed. In case the AS is given, one divides by

$$N_0 = N(E_1),$$

a tabulated number, whereas in the DS case N_0 is obtained by carrying out the last integral, setting $E = E_1$. It is then convenient to calculate dose per electron

$$D' = N_0^{-1} \int_{E_1}^{E_2} \delta(E) \phi(E) dE,$$

in the form

$$D' = \int_0^1 \delta(E) dP,$$

where for AS

$$dP = N_0^{-1} dN.$$

In the most straightforward discrete rendition, given spectral points (N_i, E_i) , the AS case produces

$$N_0 = N_1$$

$$\Delta P_i = N_0^{-1} (N_i - N_{i+1})$$

$$\delta_i = \delta((E_i + E_{i+1})/2)$$

$$D' = \sum_{i=1}^n \delta_i \Delta P_i$$

The average energy is obtained by the same method, setting δ equal to its argument. In these AS cases one notices that the energies at which dose is evaluated fall between those for which the spectrum is tabulated. These are the methods implemented in the local version of BRANDE. For each AS input, the norm, the average energy and the normalized table of ΔP_i are printed. It will be noted that by comparison with the opposite case below, in the AS case the onus of providing a decent integration (that which gives the AS) is still on the user. However this is done, the resulting average energy and dose should not be subject to much greater relative error unless there is a problem at the high energy end. Therefore the last point relative contribution to these integrals is tested and printed when it exceeds 0.1%.

Because of the more stringent requirements on the DS case, one seeks a higher order integrator (the above being zeroth order). Also because of the exponential variation, use of logarithmic steps in energy is desirable for tabulation purposes. A second order integrator⁸ using variable abscissa steps was adapted, tested and proven adequate. One such test has been to compare norm, average energy and dose at several depths for the DS and AS versions of an analytically defined steep spectrum tabulated for 101 energies. The relative norm error was less than 0.01% and that for average energy, just over 0.1%. The dose relative error ranged from 0.2% to 3.6%

for depths from 0.5 to 2.0 g/cm². The spectrum ranged from 0.1 to 5.1 MeV and averaged 0.455. The reason for higher errors in dose is that softer electrons don't reach a given depth and fewer energy points contribute to deeper depths. Thus, of the 101, the number actually contributing ranges from 84 to 36 for the same depth range. As in the AS case a test of the last point relative contribution was arranged and this indicator ranged from less than 0.1% to 2.8%. Non critical comparisons have also been made with integrators being used for these same purposes at other agencies and acceptable differences were obtained.

C. Possible Improvements

During the detailed work with the codes, two ways of improving efficiency were noted as potential help in certain kinds of production work. In case it is necessary to turn out many mass distribution graphs, the sort step is vectorizable. In case many doses are being produced, the present fixed by-pass of dose for sectors with more than 5.0 g/cm² of shielding can be made more restrictive. Selecting by-pass by an adjustable parameter relative to the dose point minimum shielding thickness would give more uniform relative errors for dose points in quite different geometries. Setting this parameter to allow dose errors right at the limit of acceptable accuracy would then result in significant time saving.

In case the main interest is near 75 mils or more all dose conversion factors below 1 MeV are zero or nearly so. This suggests another change in the present procedure. Since the main source of dose error remaining is that described at the end of the last subsection, the low energy part might be omitted, provided one uses absolute fluence rather than normalized fluence.

D. Recalibration

Recently the code SHIELDOSE⁴ has become available. It provides dose-depth calculations, given any electron or any two proton (say, solar or trapped) fluences and includes the electron bremsstrahlung. While its input information is derived from generally available sources, it is an especially convenient package for space shielding applications since it includes dose at the centers of spheres as well as two kinds of slab dose, all for omnidirectional fluence. In particular this code avoids the buildup of large variances which typically occurs in Monte Carlo electron transport codes near the end of an electron range, by separating electron and bremsstrahlung dose for later recombination. The source of SHIELDOSE electron information is ETRAN which contains all necessary physics and exhibits good comparisons with experiment. Therefore SHIELDOSE can be accepted as a physical standard for calibration purposes.

Comparison with BRANDE using the Carter fission beta spectrum⁷ in a semi-infinite slab geometry shows BRANDE to be low at nearly all depths of shielding interest and shows the discrepancy increases with depth. At 50 mils BRANDE is about 20% low and at 300 mils, about 65% low. This

discrepancy is hardly negligible and violates the hope expressed at the end of SS, Section II that BRANDE would be more accurate in relative dose comparisons. Moreover a discrepancy of this size implies that there may be a problem with the spherical calibration using SANDYL, a concern presently unresolved. For now we have decided to accept SHIELDOSE as standard and to set the SANDYL results aside.

Part of BRANDE's calculations involve the conversion of slab doses (obtained by interpolation on the TIGER input tables) to spherical sector doses for application to the sector analysis results. This conversion is by application of the Jordan factor referred to in SS, page 3. The Jordan factor involves taking a numerical derivative on the tabulated data. Since the dose-depth curve attains arbitrarily large slopes near the end of the electron range, it would be standard numerical practice to limit such numerical derivative values to avoid introducing errors. Acting on a suggestion by the originators of BRANDE,¹⁰ it was found that easing a severe restriction of the Jordan factor completely overcame the above discrepancy and allowed an agreeable comparison with SHIELDOSE. With this correction the current version of BRANDE, in the same comparison as above using 8 depths between 30 and 300 mils, shows a mean relative error of -0.4% and a standard deviation of 4%. At the same time the comparison using an earth belt spectrum² is just as good.

In detail, if the Jordan factor, F , exceeds 1, it is replaced by

$$10/(1 + 9/F),$$

a function whose value is one when F is one, which is monotonically related to F , and which never exceeds 10. Clearly this function could be much less restrictive and still satisfy the above numerical requirement. At the same time it is itself much less restrictive than the old procedure which was simply to replace F by one when it exceeded one. A number of variations were tried before settling on the above form which gives a quite adequate calibration. It should be noted that the calibration has been made for slab geometry. Besides being intuitively "geometry neutral", this geometry corresponds to the middle of the range of solid angle exposures. The discussion of the first paragraph of SS, subsection IIC implies a somewhat different evaluation of the best calibration geometry but actually was not based on as firm an understanding of the procedure as presented here. Thus BRANDE achieves any particular geometry by summing spherical sectors over all solid angle. It happens that calibrating for slab dose causes BRANDE's sphere doses to average a few percent high in the same depth comparisons as at the end of the last paragraph. The standard deviation in this comparison is twice this few percent. Should one take this average seriously, the above reasoning would suggest that a severely concave geometry would run a few percent low. Because the average is small and the deviation large, further investigation of this point would probably not be interesting. The large standard deviation occurred in calculating one ray spheres. It seems therefore that BRANDE doses benefit by the averaging process. This means that the standard deviation of the tabulated input from TIGER is significant.

The concern expressed in SS about absolute dose comparison is entirely obviated by this recalibration. Moreover since this calibration has been made for two spectra differing in average energy, errors for spectra of intermediate average energies should be of the same order as those given.

E. Proton Dose

In order to calculate proton dose in a complex geometry, the code PROTON, developed by AFWL, was translated and compared to SHIELDOSE.⁴ In this comparison PROTON averages 2 to 3% low, a sufficiently small error compared to others present to omit corrections.

III. The Effects of Calibrating BRANDE to Agree With SHIELDOSE

This recalibration results in significant change to results given in SS, Section III. The new model geometry dose-depth relations, Fig. 3, require a 135 mil shield for a factor of ten dose reduction where the old results required only 110 to 112 mils. The following table replaces the old results:

Table I. Ratio of Corner Dose to Face Dose

<u>Corner</u>	<u>50</u>	<u>Depth (mils)</u>	<u>300</u>
Dihedral	1.77		1.95
Trihedral	2.32		2.90

Thus the thumb rule: "Dihedral corners get twice the face dose and trihedral corners, three times" is seen to involve up to 30% errors, mostly at shallow depths. It is now found that the maximum dose is 52.7 Mrads which corresponds to an effective skin thickness of 91 mils. The shield needed to reduce this to 1 Mrad is 230 mils and dihedral corner shields need 22 mils less and face shields 58 mils less. The new shield then is formed simply by adding 50 mils to the four old final shield thicknesses, giving shields of 260, 230, 200 and 170 mils. This series of thicknesses was designed to take into account the 22.5 mil difference between the boxes sides and their tops. It was then necessary to make individual adjustments to 5 shields (4 of which covered non-model points) to get the dose below 1 Mrad. Final results achieved the design goal within 1% and weighed 16.46 lb. The full satellite shield weight then is 34.8 lb which is 8.7% of the satellite's weight. For thumb rule purposes one estimates a 25 Mrad average to obtain: Each power of ten dose reduction increases weight 6.2%. For comparison one could apply a 230 mil shield uniformly as before for a total weight of 85.7 lb. This gives a 60% weight savings by shielding design. The ratio attributable to model and to critical box selection would not be expected to change much, the largest part being the latter. Thus it is still true that the final shield and its weight are very sensitive to the choice of critical boxes. The detailed results follow in Figures 4 and 5 and Table II.

DOSE-DEPTH RELATIONS IN
3 MODEL GEOMETRIES,
FISSION BETA SPECTRUM
USING SECTOR-BRANDE

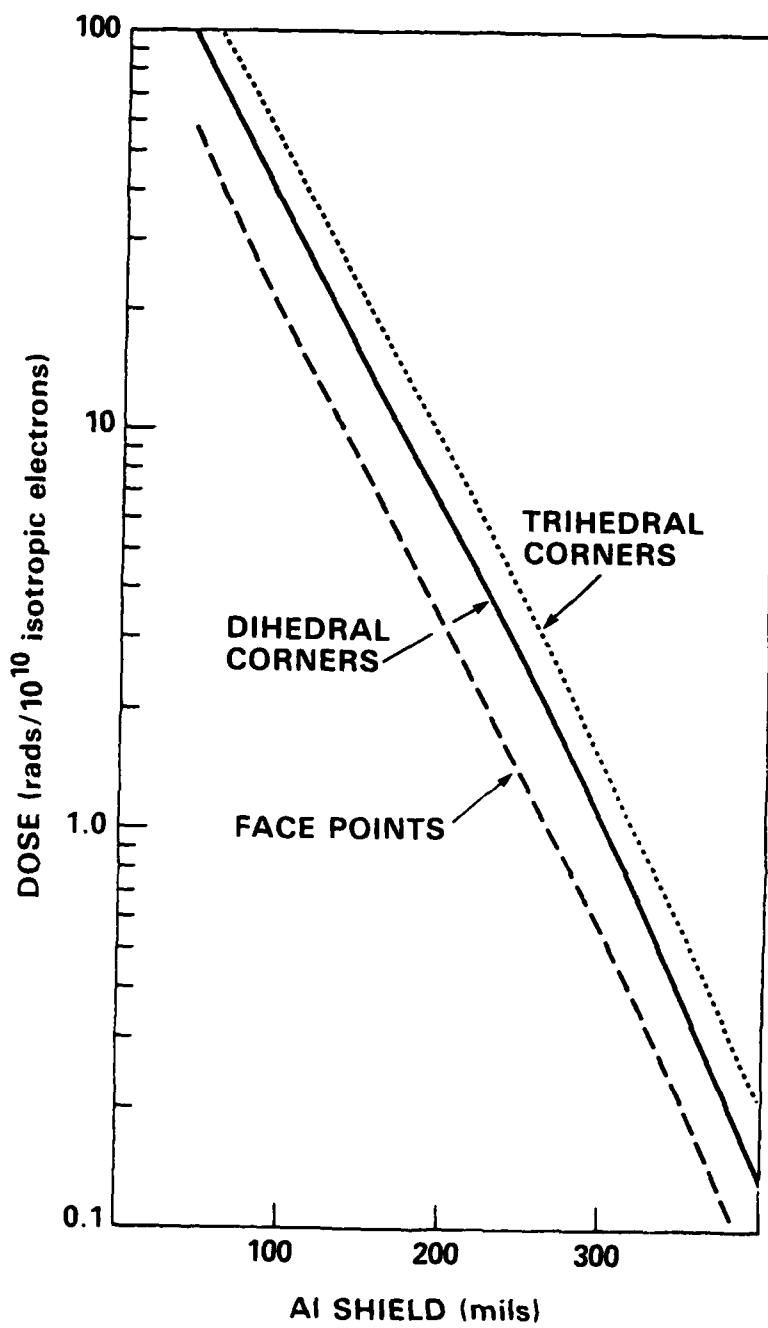


Fig. 3 — Model geometry dose-depth relations

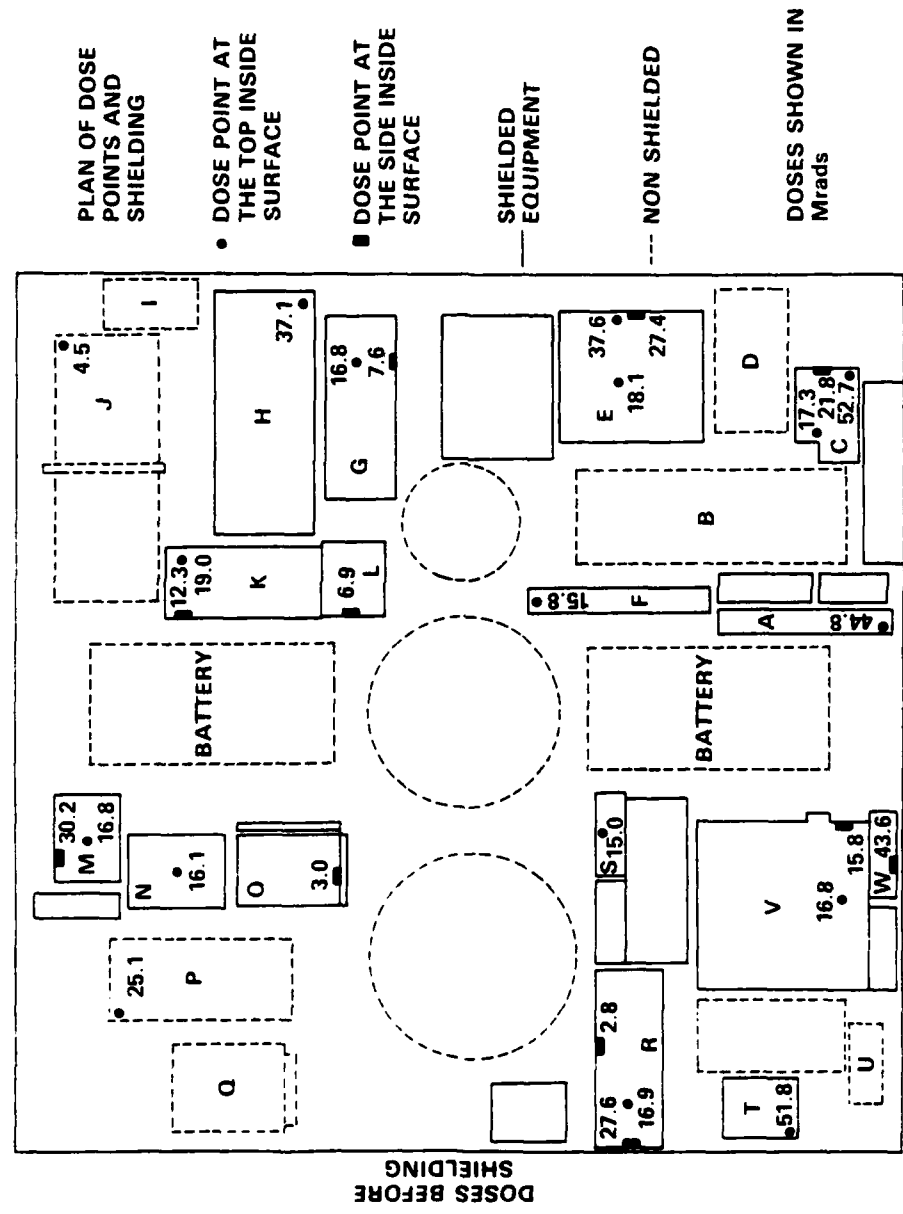


Fig. 4 — Doses before shielding

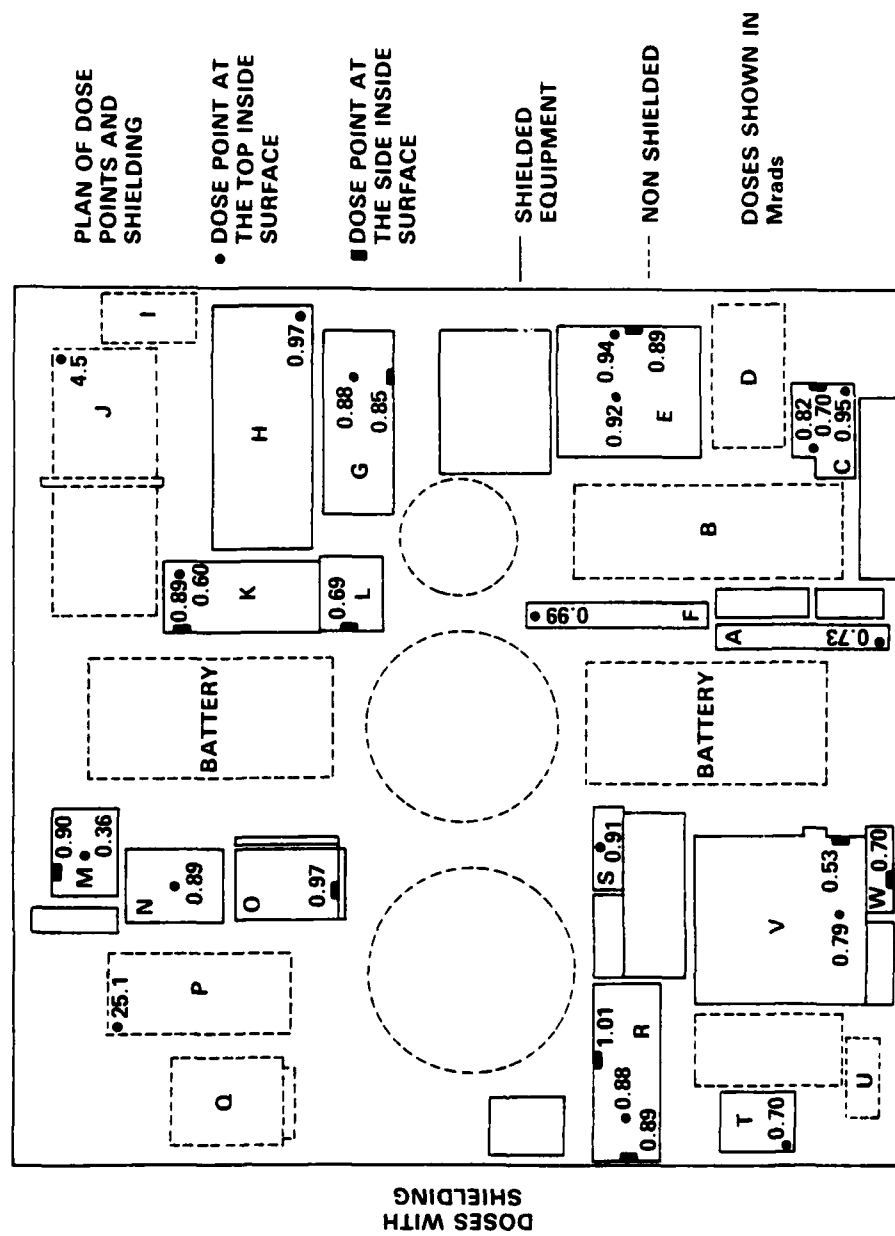


Fig. 5 — Doses with shielding

Table II. Recalibrated Doses (Mrads) at 28 Test Points

<u>Point</u>	<u>Box</u>	<u>Shield</u>		<u>Point</u>	<u>Box</u>	<u>Shield</u>	
		<u>None</u>	<u>Final</u>			<u>None</u>	<u>Final</u>
Trihedral	A	44.8	0.73	Dihedral	E	37.6	0.94
Corners	C	52.7	0.95	Corner			
	H	37.1	0.97	Top	C	17.3	0.82
	T	51.8	0.70	Faces	E	18.1	0.92
					G	16.8	0.88
					K	19.0	0.60
Side	C	21.8	0.70		N	16.1	0.89
Face	E	27.4	0.89		M	16.8	0.36
	M	30.2	0.90		R	16.9	0.88
	R	27.6	0.89		V	16.8	0.79
	W	43.6	0.70	Inside	G	7.6	0.85
Not	J	4.5	4.5	Face	K	12.3	0.89
Shielded	P	25.1	25.1		L	6.9	0.69
					O	3.0	0.97
Inside	F	15.8	0.99		R	2.8	1.01
Corner	S	15.0	0.91		V	15.8	0.53

IV. Fission Beta Shield Effectiveness Against Natural Fluences

Using the shield obtained for the fission beta spectrum in Part III, it is of interest to calculate dose reduction factors caused by this shield against the natural proton and electron fluences experienced by a satellite in a 600 nautical mile circular orbit with 63 degree inclination. Both proton and electron total fluences vary strongly with altitude so for absolute dose comparison it is quite necessary to specify the orbit. For comparison of dose reductions only this is less important since natural electron spectrum shape varies slowly with orbit parameters.

By supplying the orbit parameters and a launch date, 1981.8, spectral fluences integrated over one year have been obtained² based on the NASA earth belt fluence models AP8, AE6 and AEI7-LO. The electron spectrum so obtained is compared with the Carter fission beta spectrum⁷ and others, accumulated and normalized at 100 keV, in Figure 6. The Carter spectrum is very much harder having an average energy of 1390 keV where the natural spectrum has 247 keV. Total fluences of all electrons above 100 keV are $5.646 \times 10^{13} \text{ cm}^{-2}\text{yr}^{-1}$ and $1.0 \times 10^{16} \text{ cm}^{-2}$, respectively, the latter having been set in SS, Part III. The trapped proton spectrum so obtained extends from 2 to 500 MeV, has a total fluence of $4.8 \times 10^{10} \text{ cm}^{-2}\text{yr}^{-1}$ and an average energy of 40.4 MeV. Belt model fluences all have huge uncertainties and the two quoted here could easily vary by more than a factor of two.

The results of this exercise may be looked at from a number of different perspectives and it may be worthwhile to point out that the basic scenarios of the two radiation sources, man-made and natural, do not, of themselves, even suggest a comparison. In the case of man-made radiation, the source could be so close to the satellite that heat and blast damage are more important. Or it could be so far away as to be exceeded by natural sources in an operationally significant time. Thus the level of protection must be chosen based on such factors as consequent system degradation and overall system strategic importance. On the other hand the level of protection chosen against natural radiation may be selected based only on the expected fluences, their uncertainties, and the desired operating period in a cost-effectiveness decision. One is thus not at all surprised that on the most primitive level, that of absolute dose, there is very little in the comparison. Protection against the man-made source at the level suggested here provides a safety factor of 1000 protection against the natural source chosen for an exposure of one year. Perhaps there is more value in this comparison for what it suggests for the applicability of the shielding method used. As will be seen it suggests the method is somewhat more limited against natural than against man-made radiation.

Doses for natural spectra are presented in Table III, with and without shield, and dose reductions due to the shield are presented in Table IV. One needs to be warned that inclusion of bremsstrahlung would have increased the with-shield electron dose by from 50 to 400%. This error would be largely masked by the large proton contribution in the total dose reductions

TABLE III. SATELLITE STRUCTURE DOSES (rad/yr) FOR NATURAL SPECTRA

Type	Dose Point	Box	Trapped Protons		Trapped Electrons		Total Dose	
			no shield	shield	no shield	shield	no shield	shield
Trihedral Corner	A*		1670	968	3497	7	5167	975
	C		1803	1021	4261	11	6064	1032
	H*		1520	927	2811	14	4331	941
	T		1842	1024	4020	6	5862	1030
Dihedral Corner	E		1567	916	2847	14	4414	930
Side Face	C*		1201	795	1805	13	3006	808
	E		1258	784	2202	15	3460	799
	M		1355	827	2381	15	3736	842
	R		1318	841	2235	15	3553	856
	W*		1803	822	4588	10	6391	832
Top Face	C		1229	853	1089	13	2318	866
	E		1136	777	1142	15	2278	792
	G		978	731	1058	15	2036	746
	K		1032	646	1401	12	2433	658
	M		1266	818	1029	4	2295	822
	N		1103	761	1069	16	2172	777
	R		1149	805	1065	15	2214	820
	V		1134	771	1035	14	2169	785
Inside Corner	F		1086	770	976	33	2062	803
	S		964	671	1015	16	1979	687
Inside Face	G		734	689	478	37	1212	726
	K		825	618	780	48	1605	666
	L		755	615	398	17	1153	632
	O		757	700	155	70	912	770
	R		683	617	157	47	840	664
	V		1167	774	1089	10	2256	784
Non Shielded	J		1204	1203	134	134	1338	1337
	P		1328	1320	1857	1857	3185	3177

*Atypical, not expected to conform to class

TABLE IV. DOSE REDUCTIONS DUE TO FISSION BETA SHIELD

Type Dose Point	Box	Fission Beta	Natural Electrons	Natural Protons	Total Natural
Trihedral Corner	A*	61	468	1.73	5.30
	C	55	396	1.77	5.88
	H*	38	196	1.64	4.60
	T	74	640	1.80	5.69
Dihedral Corner	E	40	205	1.71	4.75
Side Face	C*	31	135	1.51	3.72
	E	31	142	1.60	4.33
	M	34	156	1.64	4.44
	R	31	146	1.57	4.15
	W*	62	453	2.19	7.68
Top Face	C	21	86	1.44	2.68
	E	20	75	1.46	2.88
	G	19	72	1.34	2.73
	K	32	120	1.60	3.70
	M	47	236	1.55	2.79
	N	18	69	1.45	2.80
	R	19	71	1.43	2.70
	V	21	76	1.47	2.76
Inside Corner	F	16	30	1.41	2.57
	S	16	63	1.44	2.88
Inside Face	G	9	13	1.07	1.67
	K	14	16	1.33	2.41
	L	10	23	1.23	1.82
	O	3	2	1.08	1.18
	R	3	3	1.11	1.26
	V	30	108	1.51	2.88
Non Shielded	J	1	1	1.001	1.0
	P	1	1	1.006	1.0

*Atypical, not expected to conform to class

and there it would lower them 5 to 15%. In fact the presence of protons provides the main difference from the fission beta situation. The greater penetrability of protons is reflected in the smaller variation due to geometry (the change of dose point class, excluding "non shielded", may be considered a geometry variation, from convex at the top of the tables to concave near the bottom) and in the smaller dose reductions. It needs to be noted that the with-shield proton doses would have been smaller had the equipment on the bottom of the satellite's deck been shielded, a situation safely ignored when shielding only against electrons. Significant numbers of protons penetrate the entire satellite. However the natural electrons also differ significantly from fission betas, their lower penetrability (due to a softer spectrum) showing in the higher dose reductions.

Optimizing weight in the fission beta shield design was accomplished in part by choosing the shield to uniformize (to less than but near one Mrad) the with-shield doses. An obvious trend in the natural electron with-shield doses shows that optimum design for fission beta is not optimum for this natural spectrum. An opposite trend can be observed in the proton with-shield doses but is not as remarkable.

Some consequences of proton penetrability should be noted. There is no self-shielded volume from protons for the size of satellite used here and therefore geometry models of the type in SS are not useable. The local corner character of a dose point is less relevant as may be noted by observing that the geometry classes are not as separable in proton doses. Finally it is obvious in the mediocre values of the total dose reductions that shielding is less effective in this situation than it was for fission betas. While it is effective enough against the electron component, the proton component acts as a dose floor. This is a rather clear message that there exists a natural environment against which shielding is not efficient. This situation is actually not unusual and occurs in the fission beta case as well at depths above 450 mils where bremsstrahlung provides a similar floor.

Altogether then the present exercise demonstrates that the previous shielding methods are generally applicable to natural environments but not universally efficient.

V. Device Shielding for Various Spectra

The AFWL work⁵ (HJS) most similar to SS used natural electron fluence in otherwise comparable parts while SS used man-made fluence. Thus a direct numerical comparison was not possible. One of the significant results of HJS was to compare the dose in a particular CMOS (electronics) package inside the inertial measurement unit (IMU) of a satellite with that obtained when the Kovar CMOS cover was made 10 mils thicker. The ratio of these two doses is the dose reduction factor caused by the extra 10 mils shielding and HJS obtained 1.9. The spectrum used was an extrapolation (from 2.3 to 5.0 MeV) of one obtained by Vampola for a circular polar orbit at 450 nm (nautical miles) altitude.⁶ In order to make a direct comparison, it was determined to duplicate this calculation as closely as possible. At the same time it is of interest to get dose reduction factors for several other spectra: two examples of spectra of weapon-injected electrons and two more examples of natural belt spectra. Physically one expects a smaller dose reduction for a harder spectrum, but this study provides some immediately useful numbers.

The choice of spectra for this study was made with the notion of sampling the broadest range in each class of those immediately available. As a class the weapon-injected electron fluences appear (based on a rather small sampling) to be distinctly harder than natural fluences. Of course for the purpose of obtaining dose reductions, one ignores the most distinguishing parameter of these spectra, the total fluence. The variation obtained by this selection, from hard to soft, is felt to be a fair representation of shielding from energetic electrons in the geomagnetic sphere generally. Considering the very complex problem of injection of electrons from a nuclear weapon burst at some altitude and location into a range of earth belt shells, the use of the Carter fission beta spectrum is an approximation which ignores the plasma physics of the injection process, that of interbelt diffusion, and nuclear species decay times. However AFWL has developed codes⁹ which take such effects into account and the weapon injected spectrum selected is an extreme of the small sample of AFWL results surveyed. The Carter spectrum seems representative of the softest of such spectra. On the soft side, the two natural fluence selections, while being somewhat extreme in altitude, 600 nm versus 19,323 nm, are nearly the same within their very large natural variances (factors of 2 to 10). In total fluence the average geosynchronous spectrum is a little over an order of magnitude stronger. These four spectra and that of Vampola (450 nm) are compared in Figure 6, all accumulated and normalized at the low energy end point, 0.1 MeV. It is obvious that the Vampola spectrum is a standout from the other two belt spectra. Though belt spectra natural variances are very large, even this is exceeded. This spectrum is contaminated by protons and Starfish electrons and the data were collected during a most intense few months, very unrepresentative of the remainder of that solar cycle.⁶ Moreover the extrapolation applied is not warranted for high variance data. The only purpose of using this spectrum is to make comparison with a result of HJS.

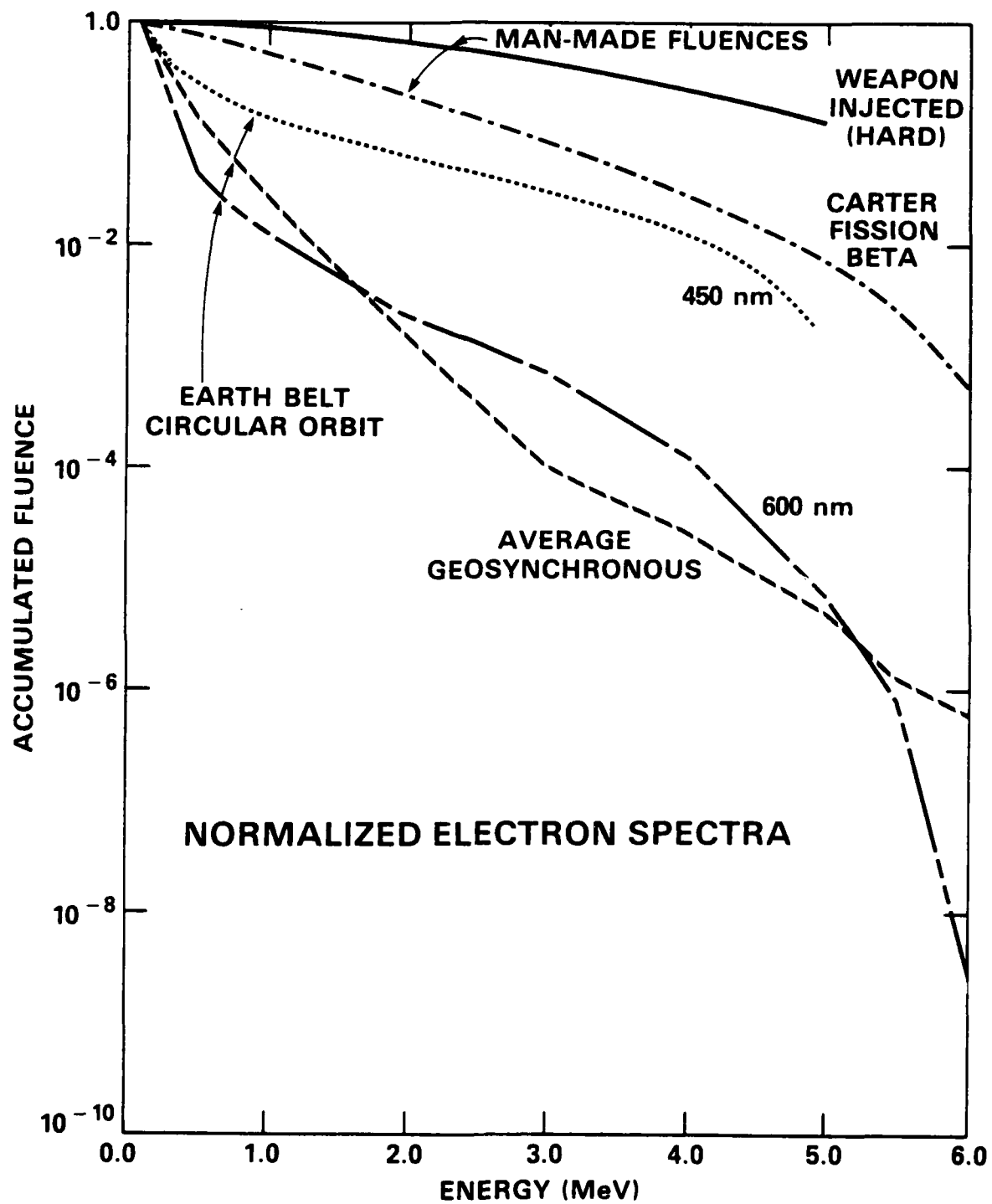


Fig. 6 — Comparison of electron spectra

It is notable that device shielding and box shielding (the method used in SS) are complementary methods and could be used together to advantage. Thus if it is known that a particular electronic device used at several places in the satellite is very radiation sensitive, it might save weight to shield it by altering its packaging, even though box shielding is also necessary.

It may be worthwhile to remark on the utility of dose reduction factors. Whenever exponential absorption applies, the elementary algebra

$$\exp(-a(2x)) = (\exp(-ax))^2$$

shows that adding another shield of the same thickness produces the same dose reduction factor as the first. Since electrons of given energy have finite ranges, this rule can only apply over some fraction of the range. In practice, especially for distributed spectra, a close approximation to exponential absorption is observed. In particular SS showed dose-depth curves for the Carter fission beta spectrum. In depths of shielding interest, the absorption exceeds pure exponential by only 20% in an order of magnitude dose reduction.

In the attempt to duplicate the HJS calculation mentioned above, previous experience indicates that it may not be necessary to duplicate their geometry but that it may be sufficient to make a mock-up geometry, observing dimensions near the dose point closely but averaging or ignoring many aspects farther away. The proof of mock-up sufficiency would then be to exhibit a mass distribution diagram resembling that of HJS rather closely. As it turned out the dose comparison achieved on this basis was sufficiently close that merely adjusting some of the assumed densities could have given a perfect comparison. This possibility occurs only because the original densities used by AFWL are not exactly known. Therefore such final adjustments are omitted, leaving the actual comparison to show what may be achieved using the mass distribution as a tool.

The geometry is a simulation of a CMOS package, ignoring the chip itself, on the exterior of a circuit board near a trihedral corner of the IMU, as in Figure 7. The IMU skin is assumed to be 60 mil aluminum. The circuit board is backed by many others and all but the first one were replaced by a homogeneous mass. Some gyros at the opposite end of the unit were replaced by a homogeneous mass. The circuit boards were given a thickness of 40 mils and a separation of 160 mils and the density was taken to be 5.0 g/cm^3 to allow for the presence of circuitry. The vertical dimensions of the CMOS package are those given by HJS: 60 mils thick with a 30 mil cylindrical central well and a 2 mil Kovar cover. The horizontal dimensions were not given so it was assumed the package was a 500 mil square and two central well diameters were used: 250 and 90 mils. Except for the Kovar cover, densities were adjusted to compensate for simulation of actual composition by aluminum. Figure 8 shows the resulting mass distribution for the 90 mil central well and the HJS result for comparison. The comparison seems adequate in the region where dose is calculated. Changing to a 250

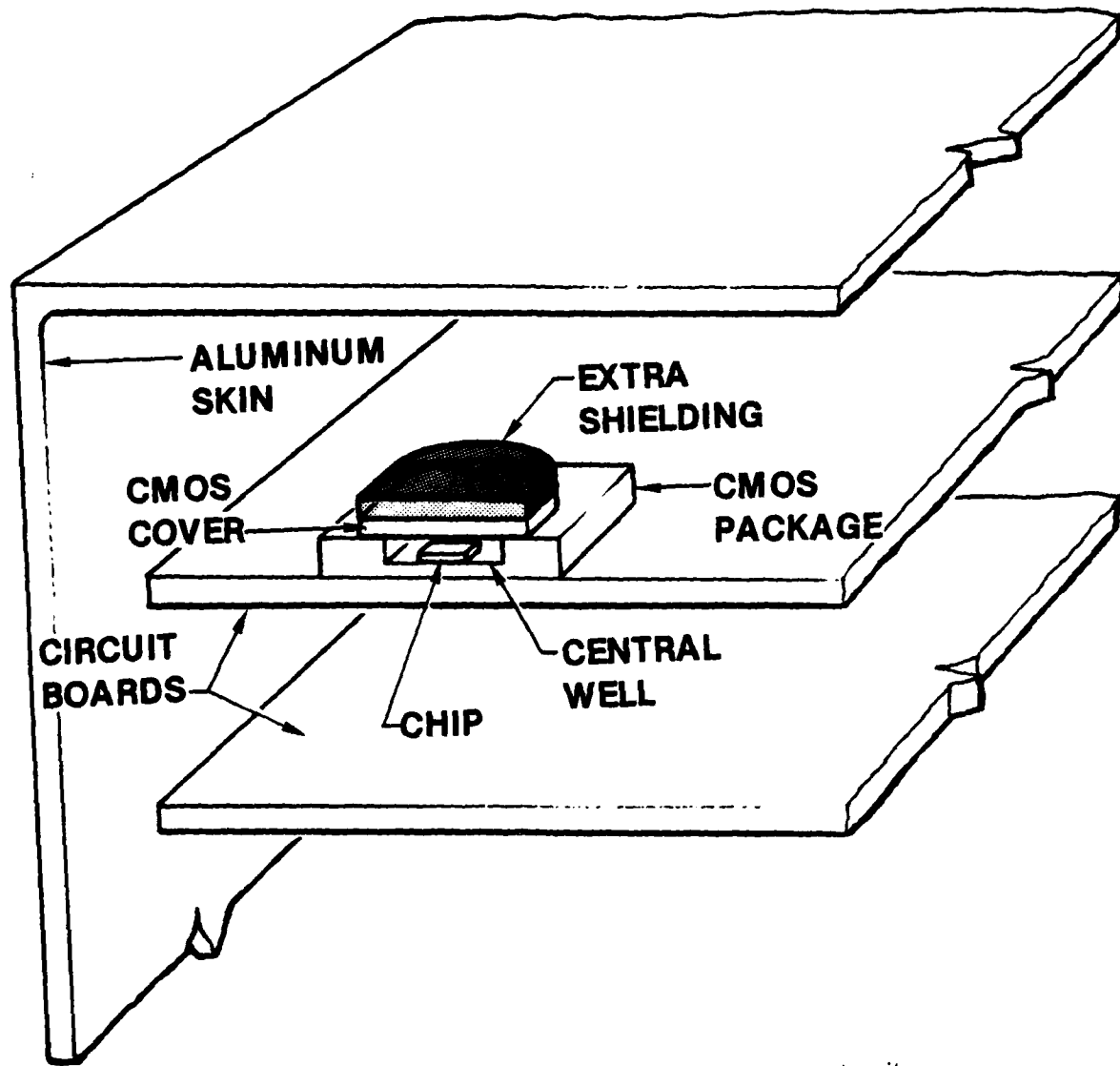


Fig. 7 — CMOS position in inertial measurement unit

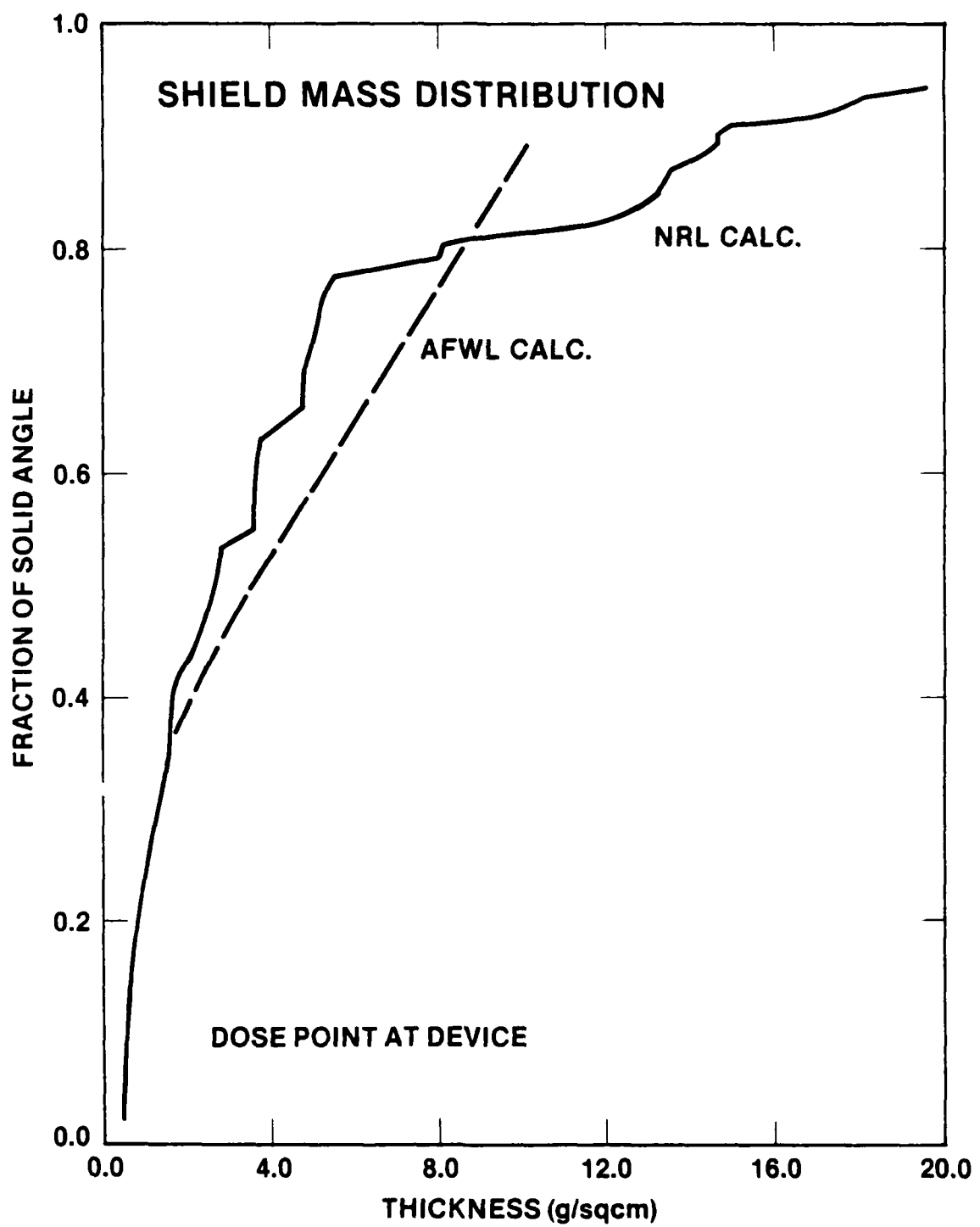


Fig. 8 — Comparison of mass distributions

mil central well moves the knee from, say, 0.35, to just above 0.4 and makes it a little more prominent, slightly worsening the agreement. However the 90 mil well seems to be an unlikely fabrication practice.

The results of the study are shown in Table V. The comparison with HJS using the 250 mil central well is 18% low, none too surprising in view of the missing dimension information. Actually some 14% is attributable directly to the new calibration of BRANDE, leaving only 4% for geometry mismatch and other unknown factors. Probably this is better than one would generally expect for this use of the mass distribution. The shift from the large to the small central well could be looked at as a 58% decrease in the solid angle contributing most of the dose if the CMOS were isolated. The fact that the results vary so little over this large geometry change means that further refinements in geometry may not contribute much. In the table this is expressed by sensitivity, that is, the relative change in dose reduction, which varies inversely with dose reduction factor. Thus this geometry change has less effect, the softer the spectrum. This is evidently because the main soft spectrum dose is more restricted by other parts of the IMU than by the edges of the central well. The fact that dose reductions do not rank obviously with the spectrum hardness is explainable because low energy electrons, below 0.9 MeV, do not penetrate the minimum shield and make no contribution to dose. Thus if these spectra were renormalized to the number of electrons above 0.9 MeV, the obvious order of their hardness then corresponds inversely to the order of dose reductions.

Table V. Device Dose Reduction Factors

<u>Spectrum</u>	<u>Dose Reductions</u>		<u>Sensitivity to Central Well Change</u>
	<u>For 250 mil Central Well</u>	<u>For 90 mil Central Well</u>	
Weapon Injected (Hard)	1.39	1.19	0.14
Carter Fission Beta	1.72	1.49	0.13
450 nm (Vampola)	1.61	1.42	0.12
600 nm	2.29	2.08	0.09
Synchronous	3.96	3.79	0.04

Acknowledgments

The author wishes to thank J. C. Ritter for sponsoring this work and J. F. Janni and G. Radke for supplying the computational tools and for many helpful conversations.

References

1. J. B. Langworthy, "A Demonstration of Satellite Shielding," NRL Memorandum Report 4275, July 22, 1980.
2. E. G. Stassinopoulos, X-601-81-7, National Space Science Data Center, Greenbelt, MD, Feb. 1981
3. E. G. Stassinopoulos, Journal of Spacecraft and Rockets, 17, 145, Mar. 1980
4. S. M. Seltzer, National Bureau of Standards Technical Note 1116, May 1980 and Radiation Shielding Information Center Code Package CCC-379.
5. D. R. Hollars, J. F. Janni and M. F. Schneider, Journal of Spacecraft and Rockets 14, 621, October 1977.
6. A. Vampola, SAMSO-TR-75-176, 1975.
7. R. E. Carter, F. Reines, J. J. Wagner and M. E. Wyman, Phys. Rev. 113, 283, 1959.
8. P. Davis & P. Rabinowitz, Methods of Numerical Integration, Academic Press 1975, p. 365.
9. J. B. Cladis, G. T. Davidson, W. E. Francis, R. K. Landshoff, and M. Walt, Improvement of SPECTER II Code: Injection and Evaluation of an Artificial Radiation Belt, AFWL-TR-78-236, August 1979.
10. G. Radke, Air Force Weapons Laboratory, private communication.